Novel [2]Catenane Structures Introducing Communication between Transition Metal Centers via $\pi\cdots\pi$ Interactions

Bohdan Korybut-Daszkiewicz,*,† Agnieszka Więckowska,‡ Renata Bilewicz,‡ Sławomir Domagała,‡ and Krzysztof Woźniak‡

Contribution from the Institute of Organic Chemistry, Polish Academy of Sciences, 01−224 Warszawa, ul. Kasprzaka 44/52, Poland, and the Chemistry Department, Warsaw University, 02−093 Warszawa, ul. Pasteura 1, Poland

Received April 2, 2001

Abstract: [2]Catenane systems containing copper(II) and nickel(II) as metal centers have been self-assembled using tetraazamacrocyclic complexes and benzo-24-crown-8 as building blocks. A variety of methods, including X-ray crystallography, ESI mass spectrometry, ^{13}C and ^{1}H NMR, and electrochemistry, were applied to characterize these new face-to-face bismacrocyclic systems. Weak $\pi\cdots\pi$ interactions introduced by interlocking transition metal complexes with benzocrown moieties were shown to increase the communication (cooperativity) of metal centers. Introduction of the benzocrown increases the stability of the mixed valence state of the macrocyclic complex, which is reflected in high values of conproportionation constants. Moreover, this effect was found to be stronger than that obtained by shortening the length of the spacer between the two tetraazamacrocyclic subunits in the parent bismacrocycles. The extent of communication is larger for the nickel catenane than for the copper one.

Introduction

Interest in molecular devices based on intertwined systems such as rotaxanes, catenanes, and helicates is connected with their fascinating architecture and potential ability to act as molecular switches, memories, catalysts, and biomimetic models.[1] Although a few simple systems with topologically nontrivial structures were synthesized with low yields using the statistical approach,[2] obtaining more complex catenanes, rotaxanes, and knots has become possible only when full capabilities of preorganization phenomena were recognized.

Strategies involving preorganization based on metal ion coordination led to several interesting molecular assemblies. In 1983, Dietrich-Buchecker and Sauvage achieved a high yield synthesis of catenanes making use of preorganization around a copper(I) template.[3] These authors introduced the term "catenate" to distinguish a metal templated catenane with an aromatic ligand providing coordination to the templating metal ion. Double stranded helicates, with oligopyridine ligands closing the tetrahedral coordination of Cu(I) and exhibiting positive cooperativity in binding of the next metal ion, were first shown by Lehn and co-workers,[4] whereas double helical binuclear complexes with the pentadentate ligand quinquepyridine were reported by Constable and co-workers.[5]

A different philosophy assumes that weak interactions should be sufficiently strong to self-assemble an ordered system, because the molecular fragments may be unable to dissociate for simple mechanical reasons after the reaction is completed.[6] Several rotaxanes and catenanes involve two organic interlocked fragments exhibiting $\pi\cdots\pi$ donor−acceptor interactions. A fairly strong interaction of a quaternary alkylated 4,4′-bipyridine unit with π-electron-rich aromatic systems was applied by Stoddart in a very efficient synthesis of interlocked molecules.[6] Hydrogen bonding[7] as well as a variety of noncovalent interactions[8] were also utilized in the processes of self-assembly. All these synthetic strategies were found useful for the construction of several catenanes and rotaxanes that can be applied in molecular devices.[1,9]

In this work, we incorporate transition metal ion tetraazamacrocyclic subunits into catenane structures. In our case, contrary to catenates prepared by Sauvage and co-workers, the metal centers are not involved in a direct coordination with the interlocked subunit (crown ether) but interact with it through strong $\pi\cdots\pi$ interactions. So far, bismacrocylic metal complexes have not been employed as building blocks of catenane systems.

† Polish Academy of Sciences.

‡ Warsaw University.

(1) Sauvage, J.-P.; Dierich-Buchecker, C. O.; Chambron, J.-C. In *Comprehensive Supramolecular Chemistry*; Lehn, J.-M., Ed.; Pergamon Press: Oxford, 1996; Vol. 9, Chapter 2. Stoddart, J. F.; Raymo, F.; Ambrillo, D. B. In *Comprehensive Supramolecular Chemistry*; Lehn, J.-M., Ed.; Pergamon Press: Oxford, 1996; Vol. 9, Chapter 3. Raymo, F. M.; Stoddart, J. F. *Chem. Rev.* **1999**, *99*, 1643−1663. Hubin, T. J.; Busch, D. H. *Coord. Chem. Rev.* **2000**, *200−202*, 5−52. Sauvage, J.-P.; Bucheker-Dietrich, C. O. *Molecular Catenanes, Rotaxanes and Knots. A Journey through the World of Topology*; Wiley: New York, 1999. Gerbeleu, N. V.; Arion, V. B.; Burges, J. *Template Synthesis of Macrocyclic Compounds*; Wiley: New York, 1999.

(2) Wasserman, E. J. *J. Am. Chem. Soc.* **1960**, *82*, 4433−4434.

(3) Dierich-Buchecker, C. O.; Sauvage, J.-P.; Kintzinger, J. P. *Tetrahedron Lett.* **1983**, *24*, 5095−5098. Dietrich-Buchecker, C. O.; Sauvage, J.-P. *Chem. Rev.* **1987**, *87*, 795−810. Dietrich-Buchecker, C. O.; Sauvage, J.-P. *Angew. Chem., Int. Ed. Engl.* **1989**, *28*, 189−192.

(4) Lehn, J.-M.; Rigault, A.; Siegel, J.; Harrowfield, J.; Chevier, B.; Moras, D. *Proc. Natl. Acad. Sci. U.S.A.* **1987**, *84*, 2565−2569.

(5) Constable, E. C.; Drew, M. G. B.; Ward, M. D. *J. Chem. Soc., Chem. Commun.* **1987**, 1600−1601.

(6) Ashton, P. R.; Goodnow, T. T.; Kaifer, A. E.; Reddington, M. V.; Slawin, A. M. Z.; Spencer, N.; Stoddart, J. F.; Vincent, C.; William, D. J. *Angew. Chem., Int. Ed. Engl.* **1989**, *28*, 1396−1399.

(7) Vögtle, F.; Meier, S.; Hoss, R. *Angew. Chem., Int. Ed. Engl.* **1992**, *31*, 1619−1622.

(8) Ismin, R.; Kaifer, A. E. *J. Am. Chem. Soc.* **1991**, *113*, 8188−8190.

(9) Balzani, V.; Credi, A.; Raymo, F. M.; Stoddart, J. F. *Angew. Chem., Int. Ed. Engl.* **2000**, *39*, 3348−3391.

10.1021/ja0108537 CCC: $20.00
Published on Web 09/01/2001

Scheme 1

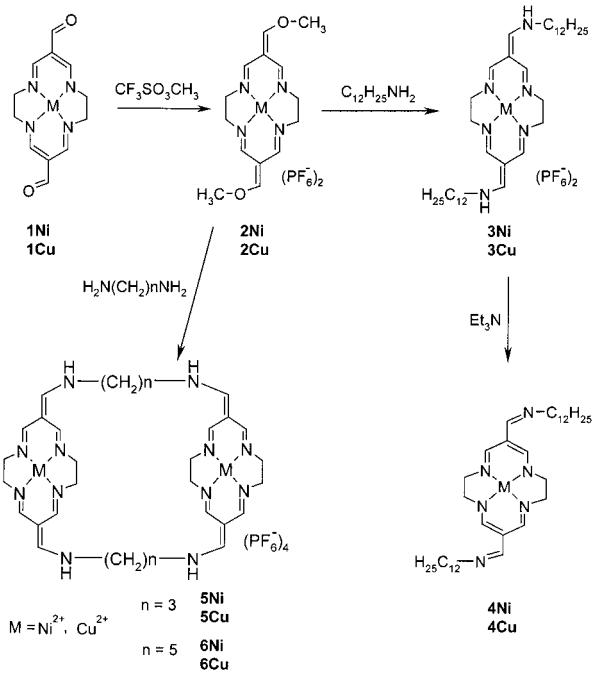

Our aim is to show that such a new design provides a possibility of modifying electronic communication between the metal centers.

We use the general Stoddart synthetic strategy based on the application of an electron-rich component (dibenzo-24-crown-8) and an electron-deficient one (in our case, unsaturated macrocyclic [14]cyclidene complexes (**2**), see Scheme 1).

Mononuclear complexes **1Ni** and **1Cu**,[10] similar to the well-known macrocyclic Schiff bases first reported by Jäger,[11] were used to obtain the bismacrocyclic compounds. We follow the Busch cyclization procedure,[12] extensively applied in the synthesis of cyclidene dioxygen carriers and face-to-face bis-macrocyclic ligands. The 14-membered tetraazamacrocycle was selected in view of its almost planar structure, which should prohibit intramolecular ring closure and favor the formation of dimeric, bismacrocyclic species (Scheme 1).

Compounds synthesized according to our strategy exhibit interesting new properties, because the weak interactions between the catenane components induce changes in the cooperativity of the metal centers. Thus, electrochemical and magnetic properties of these systems should be modified. We employ, therefore, electroanalytical techniques to follow the changes of formal potentials of the redox centers, reflecting the weak $\pi\cdots\pi$ interactions between the catenane components. Anelli and co-workers[13] demonstrated that, in [2]catenanes based on bisparaquat cyclophane, the redox centers are reduced at more negative potentials when interlocked with benzocrown ether.

(10) Grochala, W.; Jagielska, A.; Woźniak, K.; Więckowska, A.; Bilewicz, R.; Korybut-Daszkiewicz, B.; Bukowska, J.; Piela, L. *J. Phys. Org. Chem.* **2001**, *14*, 63−73. Kolchinski, A. G.; Korybut-Daszkiewicz, B.; Rybak-Akimova, E. V.; Busch, D. H.; Alcock, N. W.; Clase, H. J. *J. Am. Chem. Soc.* **1997**, *119*, 4160−4171.

(11) Jäger, E.-G. *Z. Chem.* **1968**, *8*, 392.

(12) Busch, D. H. In *Comprehensive Supramolecular Chemistry*; Lehn, J.-M., Ed.; Pergamon Press: Oxford, 1996; Vol. 9, Chapter 1. Busch, D. H.; Alcock, N. W. *Chem. Rev.* **1994,** *94*, 585−623. Hoshino, N.; Goldsby, K. A.; Busch, D. H. *Inorg. Chem.* **1986**, *25*, 3000−3006.

(13) Anelli, P. L.; Ashton, P. R.; Ballardini, R.; Balzani, V.; Delgado, M.; Gandolfi, A. E.; Goodnow, T. T.; Kaifer, A. E.; Philp, D.; Pietraszkiewicz, M.; Prodi, L.; Reddington, M. V.; Slawin, A. M.; Spencer, N.; Stoddart, J. F.; Vicent, C.; Williams, D. J. *J. Am. Chem. Soc.* **1992**, *114*, 210−214.

Scheme 2

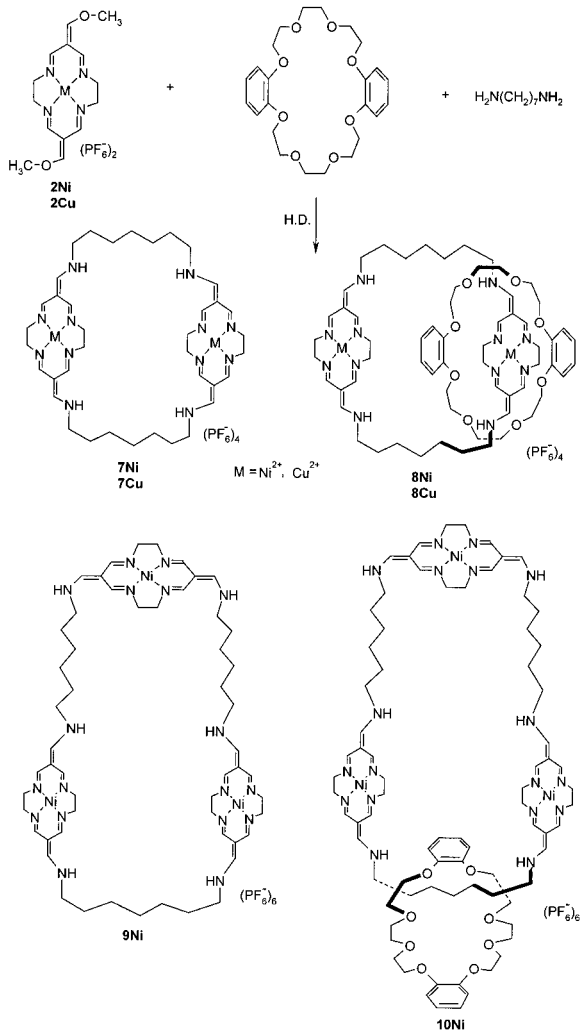

The magnitude of separation of the formal potentials of the redox sites is a measure of the extent of their electronic coupling. We expected that the catenane structure introducing additional intraunit interactions might be a way to control this coupling in the multicenter redox devices.

Results and Discussion

Synthesis and Characterization. In preliminary studies, we have found that both copper(II) and nickel(II) *O*-methylated [14]-cylidene complexes **2** (see Scheme 1) react with dodecaneamine as well as α,ω-diamines (propane-, pentane-) to form mono-cyclic amino-substituted cyclidenes (**3**) and face-to-face bis-macrocyclic dinuclear complexes (**5** and **6**), respectively. Neutral species **4Ni** and **4Cu** were also obtained by deprotonation with triethylamine in acetonitrile solution.

The reaction of the [14]cyclidene Ni^{II} complex (**2Ni)** with 1,7-heptanediamine in the presence of an excess of dibenzo-24-crown-8, carried out in acetonitrile under high-dilution conditions, afforded the bis[14]cyclidene complex (**7Ni)** and the [2]catenane complex (**8Ni)** in 30 and 15% yields, respectively (Scheme 2). A minor fraction (∼5%) consisting of the mixture of the tris[14]cyclidene complex (**9Ni)** and its [2]catenane derivative (**10Ni)** in a ∼2:1 ratio was also isolated and identified by ESI (electrospray ionization) mass spectrometry. Similar reaction with **2Cu** gave bis[14]cyclidene (**7Cu)** and [2]catenane (**8Cu)** complexes with yields of 22 and 5.5%, respectively. Higher cyclic oligomers with copper(II) were not found.

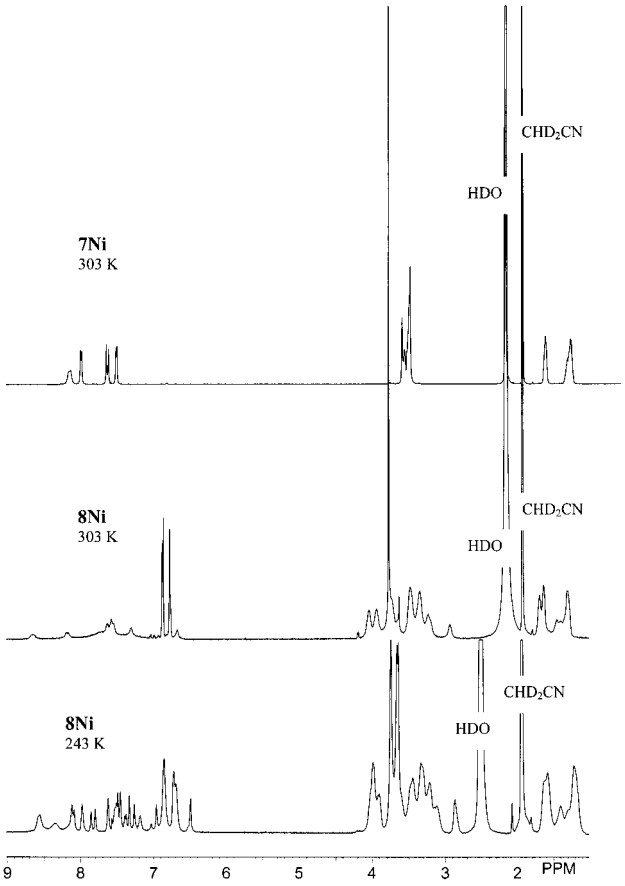

Figure 1. 500 MHz ^{1}H NMR spectra of bismacrocycle **7Ni** at 303 K and [2]catenane **8Ni** recorded at 303 and 243 K in CD_3CN solution.

Attempts to produce larger amounts of **9Ni** and **10Ni** are underway in our laboratory.

The structures of nickel(II) complexes **2Ni**−**8Ni** were established on the basis of elemental analysis as well as of ^{1}H and ^{13}C NMR and mass spectra. The ^{1}H and ^{13}C NMR spectra confirm the presence of all expected structural fragments. The spectra are broad, because of several dynamic processes occurring in the solution. The first one is caused by fast intermolecular exchange of N−H protons, resulting in the disappearance of the coupling constant with "vinyl" protons. However, in the case of monocyclic complex **3Ni** and biscyclidene complex **7Ni**, this coupling constant has been observed (15 Hz), indicating the trans ("lid-on"[14]) location of the alkyl substituent. The second process is a fast isomerization on the NMR time scale. It occurs around exocyclic (formally double) bonds and is caused by a strong coupling of the lone electron pairs of the linking nitrogens with the electron density of the unsaturated macrocyclic rings. Such an isomerism was also reported by Busch in the case of similar sixteen-member bicyclic complexes.[15] The azomethine proton signals in the spectrum of **7Ni** are split into pairs of singlets (7.50, 7.51 and 7.98, 7.99 ppm; see Figure 1), indicating the inequivalence of the two macrocyclic components of the molecule. This can be explained by cis and trans isomerism at the exocyclic carbon atoms. Although the two sides of the unsaturated chelate rings are equivalent, once the orientation at one of the exocyclic carbon atoms has been established, two orientations are then possible for the other carbon. This leads to a cis or trans orientation of the linkers. In **7Ni**, trans and cis oriented macrocyclic units are joined together to form an asymmetric dimer. The NOESY spectrum of **7Ni** at room temperature (303 K) gives similar positive NOEs between the "vinyl" protons (7.63 ppm) and all of the azomethine protons. An analogous NOE pattern is also observed for N−H protons (8.14 ppm). This indicates that the rotation of the macrocyclic fragments around the exocyclic bonds is faster than the difference between the NOE contacts, but it is obviously slow on the time scale of the chemical shift difference. Another dynamic process connected with the mutual movement of interlocked components was expected in the [2]-catenane complex (**8Ni**). Both ^{1}H (Figure 1) and ^{13}C NMR spectra of the [2]catenane complex (**8Ni**) at 303 K are broad, especially in the regions of macrocyclic chelate ring resonances. At higher temperature (333 K), three broad ^{13}C signals (invisible at room temperature) of azomethine (at 154.9 and 159.7 ppm) and exocyclic carbon atoms (at 164.0 ppm) appear. Some of the signals corresponding to the linking carbon atoms are split into pairs. This indicates that the crown ether component is localized on one of the linkers, and the macrocyclic chelate ring is too large to pass through the ether cavity.

Upon cooling (243 K), the ^{1}H NMR spectrum (Figure 1) becomes very complex in the region assigned to hydrogen atoms adjacent to unsaturated tertiary carbon and nitrogen atoms. The correlation experiment (gradient heteronuclear single quantum coherence, GHSQC) shows twelve ^{13}C signals of unsaturated tertiary carbon atoms (CH) at 153.6, 154.3, 154.4, 154.5, 158.2, 159.5, 159.6, 159.7, 162.7, 163.4, 163.9, and 167.1 ppm. However, some of the ^{13}C resonances correlate with pairs of ^{1}H signals of equal intensity. This behavior strongly suggests a simultaneous existence in solution of the two isomers, with the crown ether moiety localized around cis and trans oriented macrocyclic fragments in both ends of the molecule. The latter exists also in the solid state, which is confirmed by X-ray crystallography.

The bismacrocyclic structure of complexes **5**−**7** was confirmed by ESI mass spectrometry. The spectra of **8Ni**, the [2]-catenane complex, measured at different declustering potentials, were compared with those of the 1:1 mixture of dibenzo-24-crown-8 and **7Ni**. ESI mass spectra (see Supporting Information) of the mixture measured at low declustering potential, in addition to peaks originating from the ions of individual components, showed signals of the clusters formed from the crown ether molecule, the biscyclidene (**7Ni**) cation, and one (m/z = 465.2) or two (m/z = 770.3) PF_6^- anions. At high declustering potential, these peaks disappeared, and only signals resulting from the mixture components were observed. The ESI mass spectra of **8Ni** confirmed the [2]catenane structure. Independent of the declustering potential applied, all the peaks observed were characteristic for a molecule consisting of both components (crown ether and **7Ni**). LSIMS (liquid secondary-ion mass spectrometry) and ESI mass spectrometry of nickel and copper complexes show very similar peak patterns shifted because of the difference of the atomic masses of the coordinated metal ions.

Structural Details. The structure of the new type of catenanes based on bismacrocyclic complexes of metals (Ni^{II} and Cu^{II}) and crown ethers have been confirmed by X-ray analysis (see Experimental Section). First of all, we report on the **5Ni** bismacrocycle structure. An analogue of a PF_6^- salt of **5Ni** is used as a building block of the catenanes. Unfortunately, the higher analogues of **5Ni** do not crystallize well enough to get

(14) Busch, D. H.; Christoph, G. G.; Zimmer, L. L.; Jackels, S. C.; Grzybowski, J. J.; Callahan, R. W.; Kojima, M.; Holter, K. A.; Mocak, J.; Herron, N.; Chavan, M. Y.; Schammel, W. P. *J. Am. Chem. Soc.* **1981**, *103*, 5107−5114.

(15) Kolchinski, A. G.; Alcock, N. W.; Busch, D. H. *Inorg. Chem.* **1997**, *36*, 2754−2759.

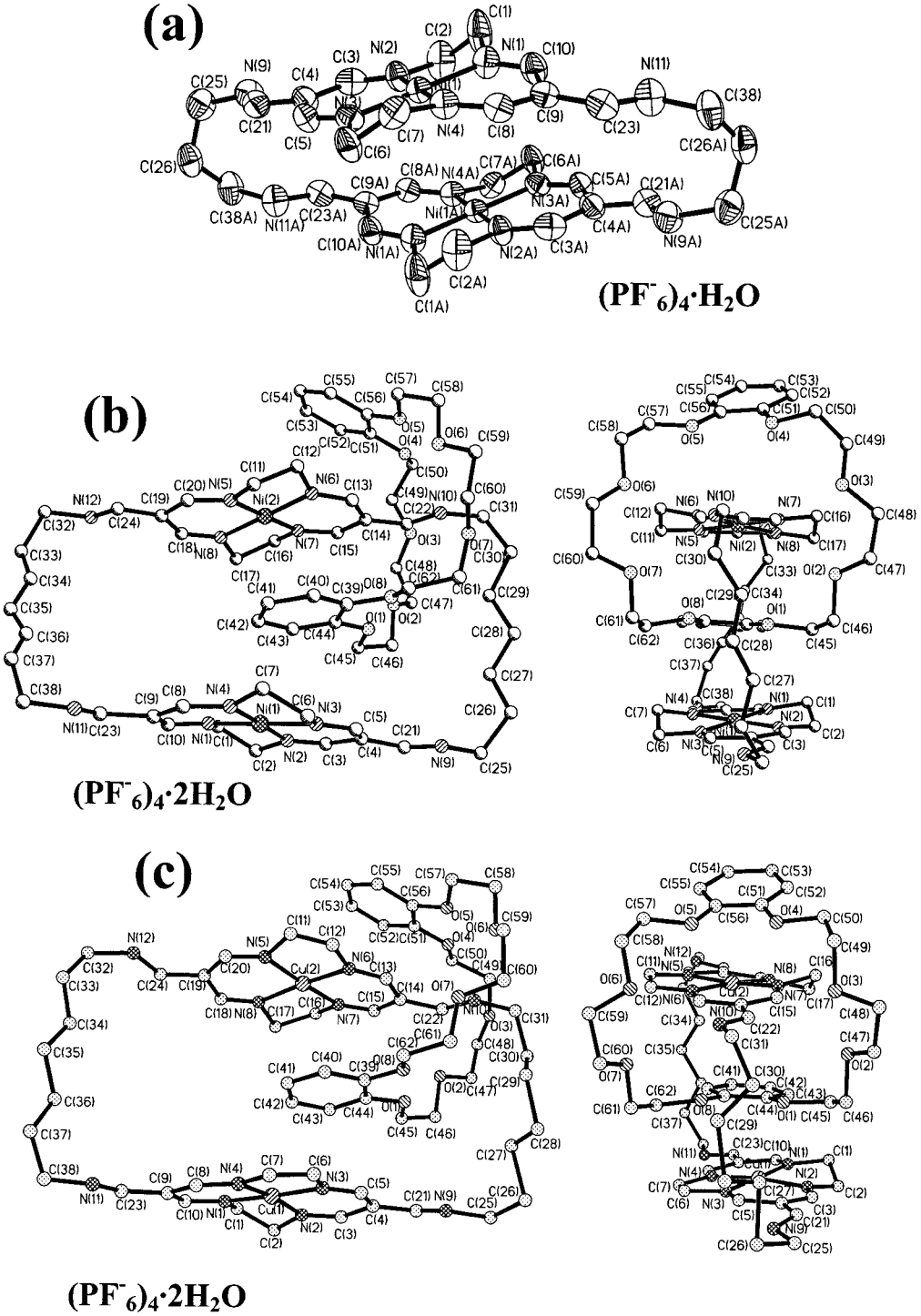

Figure 2. (a) ORTEP representation of **5Ni**, which crystallizes with four anions of PF_6^- and one molecule of H_2O, and (b,c) PLUTO illustrations of **8Ni** and **8Cu**, respectively, with the second projections on the right-hand site showing the bismacrocyclic moieties going through the crown ether. Hydrogen atoms are omitted for clarity and the counterions and water molecules represented schematically.

reasonable quality diffraction data. **5Ni** crystallizes in a special position (around a symmetry center) in the orthorhombic *Pbca* space group. From a crystallographic point of view, only half of the molecule is independent. Atoms belonging to the independent part of **5Ni** (see Figure 2) do not carry letter A in their labels.

As we can see from Figure 2, molecule **5Ni** forms nice cavities with dimensions of 4.464 Å (Ni1···Ni1A) × 14.619 Å (for C26···C26A). The size and shape of the cavity as well as the most important structural parameters are defined in Figure 3. The positively charged, coordinated to Ni^{II}, macrocyclic molecular fragments interact with each other and are slightly shifted out, thus increasing the length of the Ni···Ni nonbonding contact.

Apparently, the macrocyclic fragment is close to being planar, and its electron density seems to be conjugated with lone electron pairs of the N9 and N11 atoms. These two nitrogens form almost double bonds with the carbons attached to the macrocyclic backbone (1.287 and 1.297 Å for N9C21 and N11C38 bond lengths, respectively). The bismacrocyclic moiety interacts strongly with the closest shell of counterions and H_2O

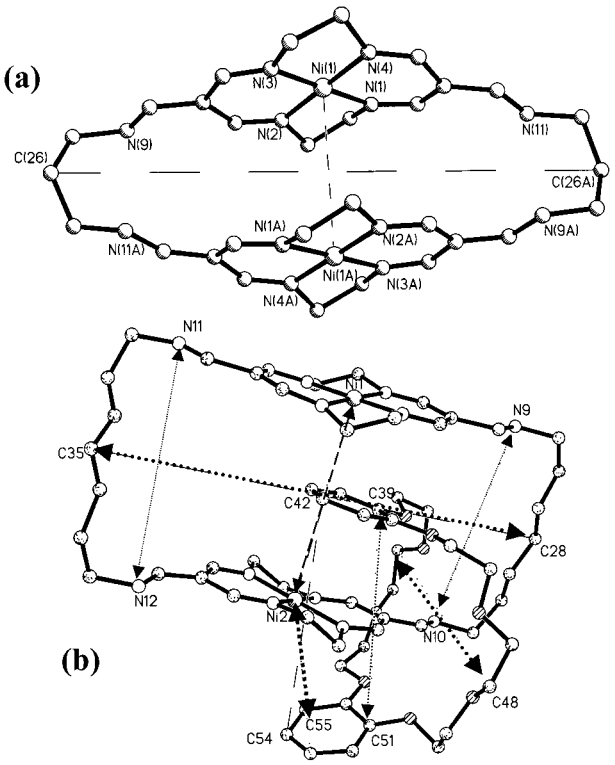

Figure 3. Definition of the sizes of molecular voids created by: (a) **5Ni**; (b) **8Ni** and **8Cu** (for numerical values, see Table 1).

Table 1. Most Important Structural Parameters. All Distances in Å

parameter definition	compound		
	8Ni	**8Cu**	**5Ni**
N11···N12	7.383	7.642	
N9···N10	7.341	6.795	N9···N11A = 3.029
C54···C41	8.208	7.525	
C28···C35	15.495	15.240	C26···C26A = 14.614
C44···C51	7.047	6.540	
M1···M2	6.743	7.066	Ni1···Ni1a = 4.464
C42···C54	8.206	7.709	
C42···M1	3.283	3.384	
C42···M2	3.470	3.883	
C54···Ni2	4.776	4.008	
C48···C60	8.894	8.414	
C39···C51	7.162	6.649	
C23···C24	6.727	7.296	C21···C23A = 3.854
C32···C38	7.268	7.538	C38···C25A = 2.563
C9···C19	6.548	7.274	C4···C9A = 4.108
C14···C4	7.056	6.820	
C21···C22	7.154	6.640	
C25···C31	7.505	6.796	

molecules. The geometrical parameters for these weak interactions and close contacts are given in Table 1.

There are four formally CH−NH−CH_2 groups (with nitrogens N9, N11, N9A, and N11A) associated with the bismacrocycle **5Ni**, two for each macrocyclic unit. Because of strong conjugation of the lone electron pairs of the nitrogen atoms with the macrocyclic electron density, these molecular fragments are more or less coplanar with the macrocycles. In doing so, they have a degree of freedom in their relative location, because each of the two CH−NH−CH_2 groups associated with a macrocyclic unit can be located either cis or trans, relative to each other. It appears that, in **5Ni**, their arrangement is trans; because of symmetry, the same is true for both macrocyclic units. The second possibility of isomerism is in the relative location of the previously mentioned amino groups, this time taken from two symmetry related bismacrocyclic units. And again, in the case of **5Ni**, a trans relative arrangement for the CH−NH−CH_2 groups located on the same hand site of the two symmetry related macrocyclic fragments is found. So, in total, there can be cis or trans isomerism both on the macrocyclic units as well as on the ends of aliphatic linkers.

In the case of catenanes, **8Ni** has cis and trans relative locations from the point of view of the macrocyclic units, and it also has these two possibilities for the CH−NH−CH_2 groups associated with the linkers (cis is the form for the linking chain located closer to the crown ether), whereas **8Cu** adopts both cis relative conformations. From this point of view, each molecule described in this paper has a slightly different conformation in the solid state.

We also want to stress that although the N9 and N11 atoms are formally neutral, they form far shorter bonds with the carbons linking them with the macrocycle (N9−C21 and N11−C23 = 1.29 Å) than with the carbons of aliphatic linkers (compared with ∼1.45 Å for N9−C25 and N11−C3). The same is true for both catenanes (∼1.14−1.34 Å for the first type of bonds and ∼1.48 Å for the bonds to the aliphatic carbons). It seems to us that the 1.14 Å bond length is definitely underestimated, probably because of X-ray data whose quality is not great.

Compound **8Ni** (Figure 2) crystallizes in the monoclinic $P2_1/c$ space group, with one molecule in the independent part of the unit cell. It consists of a few moieties, among which are two closed rings crossing each other which are interlocked: (a) a bismacrocyclic one and (b) a crown ether. Those two rings form catenane. The bismacrocyclic ring is positively charged, because of the presence of the Ni^{II} cations. This is why both interlocked rings are accompanied by four PF_6^- anions scattered around the main part of the complex. Additionally, there are two independent water molecules in structural voids formed in the crystal lattice of **8Ni** between the catenane molecules. The relative arrangement of all these moieties is illustrated in Figure 2. The structural novelty of such catenanes lies in the fact that the metallic centers in them can interact, and such interactions depend on the quality, structure, and 3D arrangement of the moieties constituting a given catenane. As we can see from Figure 2, both macrocycles in the bismacrocycle ring are slightly different.

The general pattern of the **8Cu** catenane is very close to the one for **8Ni**. It crystallizes in the monoclinic $P2_1/n$ space group with four molecules in the independent part of the unit cell. The main differences between the two catenanes are (a) a different metal ion in the macrocyclic unit, (b) different relative conformations of the CH−NH−CH_2 groups, and (c) a different planarity of the macrocyclic units (see Figure 2b,c). Let us comment on the third point. The 14-membered macrocyclic rings have two ethylene bonds (C1C2 and C6C7 or C11C12 and C16C17), which cannot fit well to the best plane of the macrocyclic fragment. So, the rings have to be perturbed out-of-plane, either in the cis or trans way. It appears that both macrocyclic rings of **8Ni** adopt cis ring conformations, whereas for **8Cu** the trans option is realized.

The crown ether in both catenanes adopts the cis conformation, located in such a manner that one of its aromatic rings goes parallel between the two metal macrocyclic units, whereas the second ring is located above one of them, however, being slightly nonparallel to the macrocycle plane. Such a relative location of both moieties resembles a sandwichlike structure, which is well illustrated in Figure 2.

In both catenanes, all M(Ni, Cu)−N bond lengths are quite typical, ranging from 1.77 to 1.89 Å for the Ni derivative and

in the range ~1.90−1.95 Å for **8Cu**. Numerical values of the most important structural parameters are given in Table 1. Also, the values of the valence angles around the central Ni^{II} ions are close to 90° (between 85 and 95°). Of course, the macrocycles are almost parallel to each other, with an angle between the best planes based on N atoms equal to 17.2°. The macrocyclic fragments with aminomethylidene ends are joined by two aliphatic chains of seven carbon atoms each. This is the reason they form a rectangular cavity of 15.40 Å (this is the distance between the C28 and C35 atoms; see Figure 3 for the definition of the most important structural parameters) × 6.71 Å (Ni1···Ni2 separation) for **8Ni** and 15.240 Å (C28···C35) × 7.066 Å (Cu1···Cu2) for **8Cu**. A great advantage of such systems from the point of view of possible applications is that the size of the cavity can easily be adjusted to the size of a guest moiety. This can be compared with the cavities obtained for similar neutral bismacrocycles.[16] For example, the size of the cavities can vary from 9.3 Å (Ni1···Ni2) × 10.1 Å (C31···C37) and 5.2 Å (Ni1···Ni1A) × 10.8 Å (C19···C19A) for similar but neutral face-to-face bismacrocyclic complexes built of 16- and 15-member units with toluene and water (water molecules stay outside the molecular voids), respectively. The first neutral complex with $CHCl_3$ has the cavity size ~10.6 Å × 7.3 Å, as we reported in our previous paper.[16] The flexibility of the cavity shape is of paramount importance for applications of such compounds. However, in the case of the positively charged systems, as discussed in this contribution, there is quite a repulsion between the charges delocalized over the macrocyclic units. This decreases the flexibility of cavity formation but, on the other hand, is an advantage, especially when an electron donating guest molecule goes between such macrocyclic charged moieties. Then, a possible charge transfer in such electron-donor−acceptor (EDA) complexes can support additional strong electrostatic interactions.

In both catenanes, the metal ions do not deviate from the best least-squares planes based on the macrocyclic nitrogen atoms. It is interesting that although there is one of the ether phenyl rings located between the macrocyclic fragments, the M^{II}···M^{II} distances in the catenanes are very short and amount to 6.743 Å for Ni1···Ni2 and 7.066 Å for Cu1···Cu2. When one compares this with the lengths of the N11···N12 and N9···N10 distances (7.38 and 7.34 Å for **8Ni**, and 7.64 and 6.80 Å for **8Cu**), it becomes obvious that there is a strong attractive interaction between the crown ether and the bismacrocycles, because the introduction of a π-electron-rich moiety between the chelated macrocycles does not increase the separation between them. The crown ether adopts strongly bent cis conformations to maximize the π···π interactions with the bismacrocycle. This means that one aromatic fragment is sandwiched by the bismacrocycle, and both of the phenyl rings of the crown ether form the other sandwich with one of the macrocycles. The angles between the best planes defined for particular molecular fragments of catenanes are given in Table 2. When one compares **5Ni** with **8Ni** or **8Cu**, it appears that despite the elongation of the linker by four C−C bonds the increase of the M^{II}···M^{II} distance amounts only to ~2.3 Å. This suggests that the presence of the benzene fragment of the ether between the macrocycles attracts them to each other.

The π···π character of the interactions within the catenane structures is also confirmed by the closest interatomic distances between atoms belonging to particular fragments of the catenanes. Such contacts are summarized in Table 2, and they range from ~3.3 Å up to 3.5 Å for **8Ni** and from 3.4 Å up to 3.9 Å for **8Cu**. This means that the aromatic ring of the crown ether is not located symmetrically between the metal ion-coordinated units, but it is slightly shifted toward the M1 (Ni1 and Cu1) ion-containing molecular fragment.

Table 2. Angles between the Best Least Square Planes Defined for the Most Important Molecular Fragments of Catenanes[a]

angle	**8Ni**	**8Cu**	**5Ni**
∠12	17.5°	3.4°	0°
∠13	12.8°	7.0°	
∠14	17.8°	22.1°	
∠23	5.4°	4.4°	
∠24	35.2°	22.8°	
∠34	30.6°	26.9°	

[a] The notation ∠12 indicates the angle between planes 1 and 2. Plane 1 includes M1, N1, N2, N3, and N4; plane 2 includes M2, N5, N6, N7, and N8; plane 3 includes C39, C40, C41, C42, C43, and C44; plane 4 includes C51, C52, C53, C54, and C56.

We want to pinpoint the role of counterions and water molecules which fill in the space between the catenane moieties. PF_6^- anions and water molecules form an outer negatively charged shell interacting mainly via electrostatic interactions with the positively charged catenane fragments. These interactions are supported by a number of weaker hydrogen-type interactions, which are numerically characterized in Tables S2−S4 and illustrated in Figures S2−S4 in the Supporting Information. Although we did not manage to find water hydrogen atom positions, the distances of the water oxygen atoms from the nearest acceptors are such that there is no doubt that the water molecules are also involved in a series of hydrogen bonds. The presence of strong electrostatic interactions and numerous hydrogen bonds is one of the reasons that these compounds crystallize well enough to collect X-ray diffraction data, allowing us to solve and refine their structures.

Electrochemistry. Monomacrocyclic complexes **3Cu** and **3Ni** exhibit close to reversible M^{II}/M^{III} electrode process (Figure 4).

In bismacrocyclic compounds, when the spacer length in the Cu^{II} and Ni^{II} complexes is increased from $n = 3$ to $n = 7$ (Table 3), the formal potentials are displaced to less positive values, denoting stronger donor abilities of the complex.

In bismacrocyclic Ni^{II} complexes, the shape of the voltammetric curve depends also on the length of the spacer. The differences between the formal potentials of both metallic centers increase when the spacer length is decreased, reflecting the increasing communication between the centers. In the case of **5Ni**, the splitting of the peaks into two indicates that the difference between the formal potentials becomes big enough for the intermediate mixed valence state to become stable.[17−19]

Comparison of the electrochemical behavior of **7Ni** and the catenane (**8Ni**) (Figure 5) reveals further strengthening of communication between the metal centers because of the mediating role of the electron-rich component, dibenzo-24-crown-8.

The linear scan and square wave voltammetry peaks of Ni^{II}/Ni^{III} in the catenane system split into two. These two new signals correspond to the sequential removal of electrons from the Ni^{II} centers. The redox behavior of molecules with multiple identical redox sites have been considered by Flanagan et al.[18] and Savéant.[20]

(16) Bilewicz, R.; Więckowska, A.; Korybut-Daszkiewicz, B.; Olszewska, A.; Woźniak, K.; Feeder, N. *J. Phys. Chem. B* **2000**, *104*, 11430−11434.

(17) Myers, R. L.; Shain, I. *Anal. Chem.* **1969**, *41*, 980−990.

(18) Flanagan, J. B.; Margel, S.; Bard, A. J.; Anson, F. C. *J. Am. Chem. Soc.* **1978**, *100*, 4248−4253.

(19) Polcyn, D. S.; Shain, I. *Anal. Chem.* **1966**, *38*, 370−375.

(20) Ammar, F.; Savéant, J.-M. *Electroanal. Chem.* **1973**, *47*, 215−221.

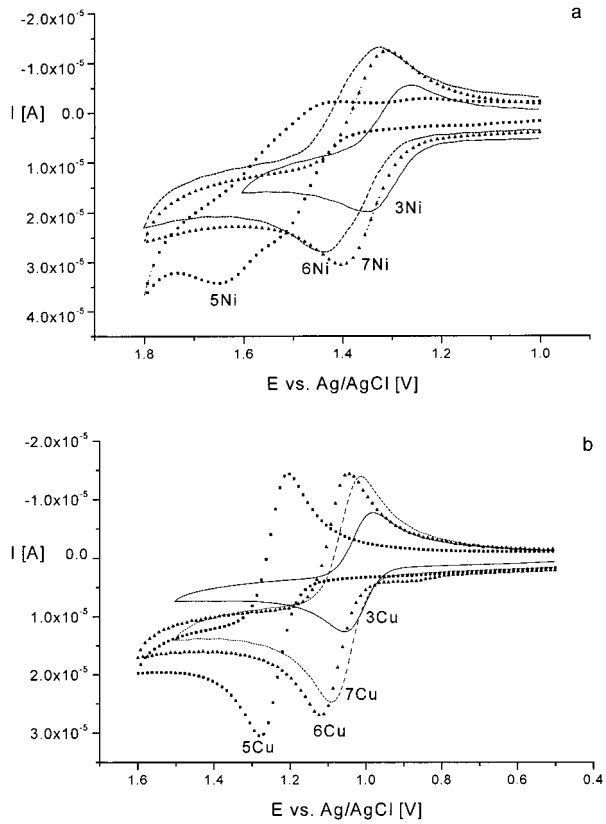

Figure 4. Cyclic voltammograms for all Ni^{II} (a) and for all Cu^{II} (b) bismacrocycles recorded using GCE in 1 mM in AN. Scan rate = 0.05 V/s.

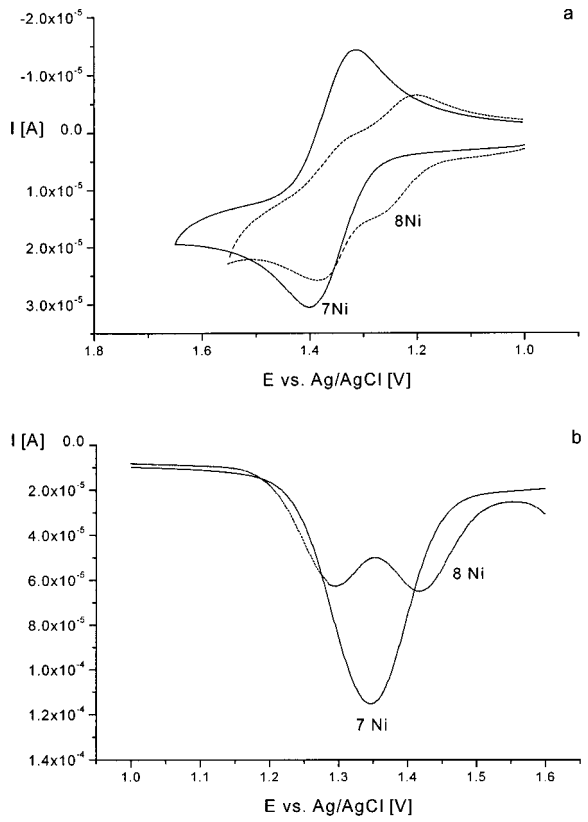

Figure 5. Cyclic and square wave voltammograms for 1 mM (a) **7Ni** and (b) **8Ni** in AN. Scan rate = 0.05 V/s; square wave frequency = 50 Hz.

Table 3. Characteristics of the M^{II}/M^{III} Electrode Process and the Values of Conproportionation Constants

compound	$E_{pa}-E_{p/2a}$ (V)	$E^0{}_1$	$E^0{}_{2'}$	ΔE^0(V)	K_{con}
3Ni	0.063	1.308			
5Ni		1.485	1.585	0.100	49.5
6Ni	0.089	1.353[a]	1.432[a]	0.079	21.7
7Ni	0.072	1.346[a]	1.417[a]	0.071	15.9
8Ni		1.391	1.250	0.141	243.0
3Cu	0.058	1.018			
5Cu	0.055	1.243		0.034	3.8
6Cu	0.057	1.084		0.037	4.3
7Cu	0.058	1.052		0.038	4.5
8Cu	0.075	1.002[a]	1.057[a]	0.055	12.4

[a] Formal potentials obtained through a fitting procedure, by means of the COOL program for the single couple of peaks corresponding to the Ni^{II}/Ni^{III} system and assuming E_1E_2 is a reversible process. E_{pa} = oxidation peak potential; $E_{p/2a}$ = half-peak potential.

The electrochemical characteristics of the Ni^{II}/Ni^{III} electrode processes in the macrocycles are shown in Table 3. The electrooxidation process corresponds to the scheme

$$Ni^{II}Ni^{II} - e \overset{E_1}{\Leftrightarrow} Ni^{II}Ni^{III} - e \overset{E_2}{\Leftrightarrow} Ni^{III}Ni^{III}$$

An additional equilibrium is the disproportionation of the Ni^{II}-Ni^{III} complex affecting the shape of the voltammogram

$$2Ni^{II}Ni^{III} \leftrightarrow Ni^{II}Ni^{II} + Ni^{III}Ni^{III}$$

where $K_{con} = \exp[(\Delta E)F/RT]$ and ΔE is the formal potential difference between the successive monoelectron transfers. For $K_{con} < 4$, ΔE is lower than 35.6 mV and the mixed valence form is unstable.[21,22] When K_{con} is equal to 4 and ΔE is 35.6 mV, the situation corresponds to completely noninteracting centers. Because of simple statistics, the difference in formal potentials of the two steps is not 0 but is equal to $(RT/nF)\ln 4$ (35.6 mV at room temperature).[21] For larger values of K_{con}, the metal centers of the system communicate with each other and the stability of the mixed valence form increases.

Interestingly, the value of the conproportionation constant increases when the interlocking crown unit is incorporated in the bismacrocyclic Ni and Cu complexes. In other words, there is already weak communication in the parent Ni bismacrocycle (**7Ni**), and this communication was strengthened by far (more than 1 order of magnitude) when the benzocrown ether unit was inserted between the Ni^{II} units (Table 3). The change of the conproportionation constant is larger than the effect of decreasing the spacer length between the tetraazamacrocyclic units in the macrocycles from seven to three methylene groups. In the case of the Cu catenane (Table 3), interlocking with benzocrown ether in fact creates communication between centers, because they are independent in the original bismacrocycle (**7Cu**).

The increase of the K_{con} from 4.54 for **7Cu** (almost noninteracting centers) to 12.40 for **8Cu** reflects increasing communication between centers (see Table 3). This suggests that designing such catenane structures may be a convenient way to induce or control the extent of communication between active centers in new multicenter redox devices.

The changes in the oxidation of the electroactive centers upon catenation were most informative; however, we also followed the changes in their reductions as well as the oxidation of crown ether itself. The reduction of the Ni^{II} and Cu^{II} bismacrocycles

(21) Gagne, R. R.; Koval, C. A.; Smith, T. J.; Cimolino, M. C. *J. Am. Chem. Soc.* **1979**, *101*, 4571−4580.
(22) Gagne, R. R.; Spiro, C. L.; Smith, T. J.; Hamann, C. A.; Thies, W. R.; Shiemke, A. K. *J. Am. Chem. Soc.* **1981**, *103*, 4073−4081.

is irreversible, with no oxidation counterparts pointing to the instability of the lower oxidation states in these complexes. For **7Ni** and **7Cu**, the reduction peaks appear at −1.407 and −1.059 V, respectively. They are also split in catenanes when the electron-rich component, dibenzo-24-crown-8, is interlocked with the bismacrocycle. This reveals that electron donation from the benzocrown unit affects the bismacrocycle unit, and the Ni^{II} center closer to it is reduced at more negative potentials than that of the parent bismacrocycle.[23]

The electron-rich component, dibenzo-24-crown-8, undergoes oxidation itself in two steps at 1.409 and 1.599 V. Upon insertion into the bismacrocycle, the hydroquinol unit oxidation is displaced toward more positive potentials and only one peak is found at 1.619 V, hence, at more positive potentials than the two signals for the benzocrown alone. This shift toward positive potentials reflects the decrease of electron density on the crown ether (weaker donor abilities), because of its interactions with the cyclidene units.

Conclusion

In conclusion, we synthesized a new type of catenane involving bismacrocyclic face-to-face complexes containing Ni^{II} and Cu^{II} ion units interacting through a $\pi\cdots\pi$ mechanism with dibenzo-24-crown-8. Contrary to catenates prepared by Sauvage and co-workers, the metal centers are not involved in a direct coordination with the interlocked subunit (crown ether) but interact with it via strong $\pi\cdots\pi$ interactions. Electron rich benzene rings of the interlocked crown ether adopt in the solid state such a conformation as to maximize donor−acceptor interactions with the bismacrocyclic subunit. Comparison of electrochemical behavior of bismacrocycles and their corresponding catenanes in the solution reveals the "mediator" role of the electron-rich component. As a result, one observes an increased communication between the metal centers reflected in the values of the conproportionation constants which are higher than in the case of the parent bismacrocyclic complexes. The extent of communication is larger for the nickel compound than for the copper one, which can be understood in terms of better π-electron accepting properties of the Ni^{II} macrocycle. This is also confirmed in the solid state by the distances between interacting units. In our opinion, such a controlled reinforcement of communication may be used in construction of multicenter redox devices.

Experimental Section

Measurements. IR spectra (paraffin oil mulls) were recorded with a Perkin-Elmer Spectrum 2000 FT-IR spectrometer. NMR spectra were measured with Bruker DRX500 Avance and Varian Gemini-200 spectrometers. Signals are reported in ppm relative to residual solvent signal. LSIMS mass spectra were obtained using an AMD 604 spectrometer, and ESI mass spectra were measured on a Mariner Perseptive Biosystem mass spectrometer.

Materials. The solvents and reagents used in these studies were reagent grade or better. Acetonitrile and dichloromethane were dried over P_2O_5 and distilled under argon. Neutral 6,13-diformyl-1,4,8,11-tetrazacyclotetradeca-4,6,12,14-tetraenato-(2-)nickel(II) and copper(II) complexes (**1Ni** and **1Cu**) were synthesized according to the previously published procedure.[10]

Synthesis. 6,13-Bis(methoxymethylidene)-1,4,8,11-tetrazacyclotetradeca-4,7,11,14-tetraene-$\kappa^4N^{1,4,8,11}$ nickel(II) Hexafluorophosphate (2Ni). Methyl trifluoromethanesufonate (*caution, toxic reagent*) (1.2 cm^3, 11 mmol) was added to a slurry of neutral [14]cyclidenenickel-(II) complex (**1Ni**) (1.52 g, 5 mmol) in dry dichloromethane (10 mL) and stirred at room temperature. After 5 h, ammonium hexafluorophosphate (5 g, 30 mmol) solution in methanol (50 mL) was added, and the reaction mixture was left in a refrigerator for crystallization. Yellow crystals of **2Ni** were filtered off, washed with methanol, and dried under reduced pressure over P_2O_5. Yield: 2.80 g, 90%. Anal. Calcd for $C_{14}H_{20}O_2N_4Ni\cdot(PF_6)_2$ (624.96): C, 26.9; H, 3.2; N, 9.0. Found: C, 26.8; H, 3.4; N, 9.0. ^{1}H NMR (200 MHz, CD_3CN): δ 4.38 (s, 3H, CH_3), 3.65 (m, 4H, CH_2-CH_2), 7.74 (s, 1H, H−C═N), 8.00 (s, 1H, H−C═N), 8.15 (s, 1H, H−C−O). ^{13}C NMR (CD_3CN, 50 MHz): δ 67.2 (CH_3), 60.0, 60.1, 60.6, 60.7 (ring CH_2-CH_2), 113.7 (ring ═C), 157.5 and 162.1 (ring H−C═N), 181.2 (═CH−O). IR (Nujol, cm^{-1}): 1659 s, 1603 vs, 839 vs, 557 s.

6,13-Bis(methoxymethylidene)-1,4,8,11-tetrazacyclotetradeca-4,7,11,14-tetraene-$\kappa^4N^{1,4,8,11}$copper(II) hexafluorophosphate (2Cu) was synthesized from neutral copper(II) complex **1Cu** following the same procedure. Yield: 90%. Anal. Calcd for $C_{14}H_{20}O_2N_4Cu\cdot(PF_6)_2$ (629.81): C, 26.7; H, 3.2; N, 8.9. Found: C, 26.5; H, 3.3; N, 8.6. IR (Nujol, cm^{-1}): 1667 s, 1620, 1600 vs, 836 vs, 558 s.

6,13-Bis(dodecylaminomethylidene)-1,4,8,11-tetrazacyclotetradeca-4,7,11,14-tetraene-$\kappa^4N^{1,4,8,11}$nickel(II) Hexafluorophosphate (3Ni). Dodecaneamine (0.185 g, 1 mmol) was added to a solution of complex **2Ni** (0.315 g, 0.5 mmol) in 25 mL of dry acetonitrile. The mixture was stirred for 4 h at room temperature, and the resulting solution was applied on a 2 cm × 20 cm acidic alumina column. The column was washed with acetonitrile. A fast-moving orange band was collected, evaporated, and crystallized from a dichloromethane−methanol solution. The orange crystalline product which precipitates upon evaporation of dichloromethane was filtered off and dried under reduced pressure. Yield: 0.39 g, 84%. Anal. Calcd for $C_{36}H_{66}N_6Ni\cdot(PF_6)_2$ (931.58): C, 46.4; H, 7.1; N, 9.0. Found: C, 46.4; H, 7.2; N, 9.2. ^{1}H NMR (CD_3CN, 200 MHz): δ 0.88 (t, J = 6.4 Hz, 3H, CH_3), 1.28 (br, 18H, aliphatic chain of nine CH_2 groups), 1.63 (q, J = 6.6 Hz, 2H, β-CH_2), 3.47 (br m, 2H, α-CH_2), 3.54 (m, 4H, ring CH_2-CH_2), 7.50 and 8.00 (both s, 1H, ring N═C−H), 7.64 (d, J = 15.0 Hz, 1H, C═CH−N), 8.23 (br d, J = 15.0 Hz, 1H, N−H). ^{13}C NMR (CD_3CN, 50 MHz): δ 14.4 (CH_3), 23.4, 26.8, 29.7, 30.0, 30.1, 30.2, 30.3 × 3, 32.6 and 51.7 (aliphatic chain CH_2), 59.3, 59.5, 60.2, 60.4 (ring CH_2-CH_2), 104.1 (ring ═C), 155.1 and 160.6 (ring H−C═N), 163.9 (═CH−N). IR (Nujol, cm^{-1}): 3381 s, 1672 s, 1635 vs, 1557 s, 831 vs, 555 s. MS (LSIMS, NBA, *m*/*z*): 639 ($[C_{36}H_{66}N_6Ni]^{2+} - H^+$). MS (ESI, CH_3CN, *m*/*z*): 320.5 ($[C_{36}H_{66}N_6Ni]^{2+}$), 639.5 ($[C_{36}H_{66}N_6Ni]^{2+} - H^+$), 785.6 ($[C_{36}H_{66}N_6Ni]^{2+} + PF_6^-$).

6,13-Bis(dodecylaminomethylidene)-1,4,8,11-tetrazacyclotetradeca-4,7,11,14-tetraene-$\kappa^4N^{1,4,8,11}$copper(II) hexafluorophosphate (3Cu) was synthesized from copper(II) complex **2Cu** following the same procedure. Yield: 85% of red crystals. Anal. Calcd for $C_{36}H_{66}N_6Cu\cdot(PF_6)_2$ (936.43): C, 46.2; H, 7.1; N, 9.0. Found: C, 46.1; H, 7.2; N, 8.9. IR (Nujol, cm^{-1}): 3387 s, 1669 s, 1639 vs, 1573 s, 833 vs, 557 s. MS (LSIMS, NBA, *m*/*z*): 644 ($[C_{36}H_{66}N_6Cu]^{2+} - H^+$).

6,13-Bis(dodecyliminomethylidene)-1,4,8,11-tetrazacyclotetradeca-4,6,12,14-tetraenato-(−2)-$\kappa^4N^{1,4,8,11}$nickel(II) (4Ni). Triethylamine (0.1 mL, 0.8 mmol) was added to a solution of complex **3Ni** (0.186 g, 0.2 mmol) in acetonitrile (10 mL). Precipitated dark orange solid was filtered off and recrystallized from dichloromethane−acetonitrile solution. Yield: 0.11 g, 86%. Anal. Calcd for $C_{36}H_{64}N_6Ni$ (639.63): C, 67.6; H, 10.1; N, 13.1. Found: C, 67.3; H, 10.0; N, 13.4. ^{1}H NMR ($CDCl_3$, 200 MHz): δ 0.88 (t, J = 6.5 Hz , 3H, CH_3), 1.26 (br, 18H, aliphatic chain of nine CH_2 groups), 1.56 (q, J = 6.5 Hz, 2H, β-CH_2), 3.33 (t, J = 7.0 Hz, 2H, α-CH_2), 3.35 (s, 4H, ring CH_2-CH_2), 7.47 (s, 2H, ring N═C−H), 7.72 (s, 1H, C═CH−N). ^{13}C NMR ($CDCl_3$, 50 MHz): δ 14.1 (CH_3), 22.7, 27.4, 29.4, 29.5, 29.6 × 4, 31.7, 31.9 and 61.4 (aliphatic chain CH_2), 58.5 (ring CH_2-CH_2), 105.5 (ring ═C), 153.6 × 2 (ring H−C═N), 159.8 (═CH−N). IR (Nujol, cm^{-1}): 1633 w, 1605 vs, 1520 s. MS (LSIMS, NBA, *m*/*z*): 639 ($[C_{36}H_{64}N_6Ni] + H^+$). MS (ESI, CH_3CN, m/z): 320.5 ($[C_{36}H_{64}N_6Ni] + 2H^+$), 639.5 ($[C_{36}H_{64}N_6Ni] + H^+$).

6,13-Bis(dodecyliminomethylidene)-1,4,8,11-tetrazacyclotetradeca-4,6,12,14-tetraenato-(−2)-$\kappa^4N^{1,4,8,11}$copper(II) (4Cu) was synthesized from copper(II) complex **3Cu** following the same procedure. Yield: 85% of green crystals. Anal. Calcd for $C_{36}H_{64}N_6Cu$ (644.49): C, 67.1;

(23) Kaifer, A. E.; Gómez-Kaifer, M. *Supramolecular Electrochemistry*; Wiley-VCH: Weinheim, 1999, pp 94−102.

H, 10.0; N, 13.0. Found: C, 67.0; H, 10.0; N, 13.1. IR (Nujol, cm^{-1}): 1635 w, 1602 vs, 1541 s. MS (LSIMS, NBA, *m*/*z*): 644 ($[C_{36}H_{64}N_6Cu] + H^+$).

(3,7,11,14,18,22,26,29,32,35,38,41-Dodecaazatricyclo[22.6.6.6^{9,16}]dotetraconta-1,8,10,14,16,23,25,29,31,35,37,41-dodecaene-κ^8N)dinickel(II) Hexafluorophosphate (5Ni). 1,3-Propylenediamine (0.074 g, 1 mmol) was added to a solution of complex **2Ni** (0.63 g, 1 mmol) in 50 mL of dry acetonitrile. The mixture was stirred for 16 h at room temperature, after which 2 mL of concentrated hydrochloric acid was added. An orange precipitate was filtered off and dissolved in water (50 mL), and the resulting solution was absorbed on a 2 cm × 20 cm SP Sephadex C-25 column. The column was washed with water and eluted with 0.5 M NaCl solution. The major orange band was collected and the product precipitated upon addition of ammonium hexafluorophosphate (5 g). The precipitate was filtered off, dissolved in acetonitrile containing a small amount of ammonium hexafluorophosphate, and diluted with ethanol. An orange product precipitated upon slow evaporation of acetonitrile was filtered off, washed with ethanol, and dried under reduced pressure. The crystals for X-ray structural analysis were obtained by slow evaporation of an acetone−water solution of **3**. Yield: 0.25 g, 39%. Anal. Calcd for $C_{30}H_{44}N_{12}Ni_2\cdot(PF_6)_4\cdot H_2O$ (1288.01): C, 28.0; H, 3.6; N, 13.0. Found: C, 27.9; H, 3.7; N, 12.9.^{1}H NMR (CD_3CN, 500 MHz): δ 2.09 (br m, 4H, β-CH_2), 3.66 (br m, 24H, α-CH_2 and ring CH_2—CH_2), 7.68 (v br, 8H, ring N═C—H), 7.70 (br s, 4H, C═CH—N), 7.90 (v br, 4H, NH). ^{13}C NMR (CD_3CN, 125 MHz): δ 28.0, 51.0 (linker CH_2), 59.6 (br, ring CH_2—CH_2), 104.7 (ring ═C), 154.8 and 160.5 (both br, ring HC═N), 164.0 (═CH—N). IR (Nujol, cm^{-1}): 3651 s, 3585 w, 3370 m, 3224 w, 1660 s, 1625 vs, 1580 s, 845 vs, 559 s. MS (LSIMS, NBA, *m*/*z*): 343 ($[C_{30}H_{44}N_{12}Ni_2]^{4+} - 2H^+$), 685 ($[C_{30}H_{44}N_{12}Ni_2]^{4+} - 3H^+$), 831 ($[C_{30}H_{44}N_{12}Ni_2]^{4+} - 2H^+ + PF_6^-$), 977 ($[C_{30}H_{44}N_{12}Ni_2]^{4+} - H^+ + 2PF_6^-$), 1123 ($[C_{30}H_{44}N_{12}Ni_2]^{4+} + 3PF_6^-$). MS (ESI, CH_3CN, *m*/*z*): 343.3 ($[C_{30}H_{44}N_{12}Ni_2]^{4+} - 2H^+$), 352.4 ($[C_{30}H_{44}N_{12}Ni_2]^{4+} - 2H^+ + H_2O$).

(3,7,11,14,18,22,26,29,32,35,38,41-Dodecaazatricyclo[22.6.6.6^{9,16}]dotetraconta-1,8,10,14,16,23,25,29,31,35,37,41-dodecaene-κ^8N)dicopper(II) hexafluorophosphate (5Cu) and (3,9,13,16,20,26,30,33,37,40,42,45-dodecaazatricyclo[26.6.6.6^{11,18}]hexatetraconta-1,10,12,16,18,27,29,33,35,39,41,45-dodecaene-κ^8N)dicopper(II)] hexafluorophosphate (**6Cu**) were synthesized from copper(II) complex **2Cu** following the same procedure and purified by crystallization from an acetonitrile−water solution.

5Cu. Anal. Calcd for $C_{30}H_{44}N_{12}Cu_2\cdot(PF_6)_4\cdot H_2O$ (1279.71): C, 27.8; H, 3.6; N, 13.0. Found: C, 27.7; H, 3.6; N, 12.9. IR (Nujol, cm^{-1}): 3652 s, 3585 w, 3378 m, 3238 w, 1660 w, 1627 vs, 1588 s, 844 vs, 559 s. MS (LSIMS, NBA, *m*/*z*): 349 ($[C_{30}H_{44}N_{12}Cu_2]^{4+} - 2H^+$), 695 ($[C_{30}H_{44}N_{12}Cu_2]^{4+} - 3H^+$), 841 ($[C_{30}H_{44}N_{12}Cu_2]^{4+} - 2H^+ + PF_6^-$), 987 ($[C_{30}H_{44}N_{12}Cu_2]^{4+} - H^+ + 2PF_6^-$), 1133 ($[C_{30}H_{44}N_{12}Cu_2]^{4+} + 3PF_6^-$).

6Cu. Anal. Calcd for $C_{34}H_{52}N_{12}Cu_2\cdot(PF_6)_4$ (1335.82): C, 30.6; H, 3.9; N, 12.6. Found: C, 30.4; H, 4.1; N, 12.6. IR (Nujol, cm^{-1}): 3363 m, 1660 w, 1621 vs, 1581 s, 847 vs, 559 s. MS (LSIMS, NBA, *m*/*z*): 751 ($[C_{34}H_{52}N_{12}Cu_2]^{4+} - 3H^+$), 897 ($[C_{34}H_{52}N_{12}Cu_2]^{4+} - 2H^+ + PF_6^-$), 1043 ($[C_{34}H_{52}N_{12}Cu_2]^{4+} - H^+ + 2PF_6^-$), 1189 ($[C_{34}H_{52}N_{12}Cu_2]^{4+} + 3PF_6^-$).

(3,9,13,16,20,26,30,33,37,40,42,45-Dodecaazatricyclo[26.6.6.6^{11,18}]hexatetraconta-1,10,12,16,18,27,29,33,35,39,41,45-dodecaene-κ^8N)dinickel(II) Hexafluorophosphate (6Ni). 1,5-Pentanediamine (0.102 g, 1 mmol) was added to a solution of complex **2** (0.63 g, 1 mmol) in 50 mL of dry acetonitrile. The mixture was stirred for 16 h at room temperature, and the resulting solution was applied on a 2 cm × 20 cm acidic alumina column. The column was washed with acetonitrile. The fast-moving orange band was collected, evaporated, and crystallized from acetonitrile (5 mL) solution. The orange crystalline product was filtered off and dried under reduced pressure. Yield: 0.32 g, 48%. Complex **6Ni** precipitated on the SP Sephadex C-25 column and therefore could not be purified by ion exchanging chromatography. Anal. Calcd for $C_{34}H_{52}N_{12}Ni_2\cdot(PF_6)_4$ (1326.10): C, 30.8; H, 4.0; N, 12.7. Found: C, 30.8; H, 4.1; N, 12.6. ^{1}H NMR (CD_3CN, 500 MHz): δ 1.35 (m, 4H, γ-CH_2), 1.66 (m, 8H, β-CH_2), 3.53 (m, 8H, α-CH_2), 3.65 (br m, 16H, ring CH_2—CH_2), 7.48 (br s, 4H, ring N═C—H), 7.91 (br s, 4H, ring N═C—H), 7.62 (s, C═CH—N), 8.40 (br s, 4H, NH). ^{13}C NMR (CD_3CN, 125.4 MHz): δ 22.2, 28.6, 51.3 (linker CH_2), 59.7 and 60.5 (both br, ring CH_2—CH_2), 104.0 (ring ═C), 155.2 and 161.0 (both br, ring HC═N), 164.7 (═CH—N). IR (Nujol, cm^{-1}): 3372 m, 1661 s, 1625 vs, 1577 s, 849 vs, 560 s. MS (LSIMS, NBA, *m*/*z*): 371 ($[C_{34}H_{52}N_{12}Ni_2]^{4+} - 2H^+$), 444 ($[C_{34}H_{52}N_{12}Ni_2]^{4+} - H^+ + PF_6^-$), 517 ($[C_{34}H_{52}N_{12}Ni_2]^{4+} + 2PF_6^-$), 741 ($[C_{34}H_{52}N_{12}Ni_2]^{4+} - 3H^+$), 887 ($[C_{34}H_{52}N_{12}Ni_2]^{4+} - 2H^+ + PF_6^-$), 1033 ($[C_{34}H_{52}N_{12}Ni_2]^{4+} - H^+ + 2PF_6^-$), 1179 ($[C_{34}H_{52}N_{12}Ni_2]^{4+} + 3PF_6^-$).

(3,11,15,18,22,30,34,37,41,44,46,49-Dodecaazatricyclo[26.6.6.6^{13,20}]pentaconta-1,12,14,18,20,31,33,37,39,43,45,49-dodecaene-κ^8N)dinickel(II) Hexafluorophosphate (7Ni) and (3,11,15,18,22,30,34,37,41,44,46,49-Dodecaazatricyclo[26.6.6.6^{13,20}]pentaconta-1,12,14,18,20,31,33,37,39,43,45,49-dodecaene-κ^8N)dinickel(II)-dibenzo-24-crown-8[2]catenane Hexafluorophosphate (8Ni). 1,7-Heptanediamine (0.130 g, 1 mmol) and complex **2Ni** (0.625 g, 1 mmol) were separately dissolved in 100 mL of dry acetonitrile containing 0.448 g (1 mmol) dibenzo-24-crown-8. These two solutions were added at a rate of 15 $cm^3\ h^{-1}$, by means of a peristaltic pump, to a stirred solution of dibenzo-24-crown-8 (0.448 g, 1 mmol) in acetonitrile (100 mL). After the addition was complete, the solvent was removed by rotary evaporation to give a dark orange residue. The residue was then washed out on the top of a 2 cm × 25 cm silica (Merck, 70−230 mesh) column with several small portions of chloroform. The column was washed with chloroform until all excessive crown ether was collected (∼1.2 g). The solid remaining on the top of the column was then dissolved with a small volume of acetonitrile and eluted with the same solvent. The orange eluate was evaporated to dryness, and the solid was extracted several times with methanol. The solid was then dissolved in acetonitrile and applied on a 2 cm × 15 cm acidic alumina column (Merck, activity I) and eluted with acetonitrile. A fast moving yellow band was collected, concentrated, and diluted with water. The orange cyclophane (**7**), precipitated upon evaporation of acetonitrile, was filtered off, washed with methanol and chloroform, and dried in vacuo. Yield: 0.202 g, 30%. The methanol solution was evaporated to dryness and the residue dissolved in acetonitrile and passed through a 2 cm × 15 cm acidic alumina column (Merck, activity I). The first yellow fraction of **8Ni** eluted with acetonitrile and, after evaporation, was dissolved in dichloromethane containing 5% of methanol and diluted with chloroform. An orange precipitate of [2]catenane (**8Ni**) formed upon evaporation of dichloromethane was filtered off, washed with chloroform, and dried in vacuo. Yield: 0.140 g, 15%. Crystals for X-ray structural analysis were obtained by slow evaporation of an acetonitrile−ethanol solution of **8Ni**. The second, orange fraction (**9Ni** + **10Ni**) was eluted with a methanol−acetonitrile 1:10 solution and after partial evaporation precipitated upon addition of water. Yield: 0.048 g.

7Ni. Anal. Calcd for $C_{38}H_{60}N_{12}Ni_2\cdot(PF_6)_4$ (1382.21): C, 33.0; H, 4.4; N, 12.1. Found: C, 33.6; H, 4.6; N, 11.8. ^{1}H NMR (500 MHz, CD_3CN): δ 1.22−1.35 (m, 12H, γ- and δ-CH_2), 1.62 (m, 8H, β-CH_2,) 3.49 (br s, 8H, α-CH_2), 3.45−3.61 (m, 16H, en-CH_2), 7.50 (s, 2H, H—C═N), 7.51 (s, 2H, H—C═N), 7.63 (d, J = 15 Hz, 4H, H—C—N), 7.98 (s, 2H, H—C═N), 7.99 (s, 2H, H—C═N), 8.14 (br m, 4H, N—H). ^{13}C NMR (CD_3CN, 125.4 MHz): δ 29.6, 26.8, 30.1, 51.8 (linker CH_2), 59.9 (br, ring CH_2—CH_2), 104.1 (ring ═C), 155.1 and 161.7 (both br, ring HC═N), 164.1 (═CH—N). IR (Nujol, cm^{-1}): 3384, 1663 s, 1620 vs, 1567, 843 vs, 557 s. MS (ESI, CH_3CN, *m*/*z*): 200.6 ($[C_{38}H_{60}N_{12}Ni_2]^{4+}$), 267.1 ($[C_{38}H_{60}N_{12}Ni_2]^{4+} - H^+$), 315.1 ($[C_{38}H_{60}N_{12}Ni_2]^{4+} + PF_6^-$), 545.1 ($[C_{38}H_{60}N_{12}Ni_2]^{4+} + 2PF_6^-$).

8Ni. Anal. Calcd for $C_{62}H_{92}O_8N_{12}Ni_2\cdot(PF_6)_4\cdot 2H_2O$ (1866.76): C, 39.9; H, 5.2; N, 9.0. Found: C, 39.7; H, 5.4; N, 9.0. ^{1}H NMR (500 MHz, CD_3CN): δ 1.15−1.45 (br m, 12H, γ- and δ-CH_2), 1.66 (br, 8H, β-CH_2), 2.90−3.60 (br m, 24H, α-CH_2 and en-CH_2), 3.78 (s, 8H, center O—CH_2—CH_2—O), 3.65−3.80 (br m, 8H, CH_2—O), 3.95 and 4.05 (both br, both 4H, Ph—O—CH_2), 6.78 and 6.88 (m, 8H, aromatic protons), 6.60−8.70 (several, br, 16H, H—C═N and N—H). ^{13}C NMR (CD_3CN, 125.4 MHz, 333 K): δ 30.1, 30.6, 27.1, 27.2, 30.4 × 2, 52.1 × 2 (br, linker CH_2), 59.7 (v br, ring CH_2—CH_2), 104.6 and 104.7 (ring ═C), 154.9 and 159.7 (both v br, ring HC═N), 164.0 (v br, ═CH—N), 69.0, 71.4, 71.8 (O—CH_2—CH_2—O), 113.3 (α-Ph), 122.2 (β-Ph), 149.5 (O—Ph). IR (Nujol, cm^{-1}): 3367, 1660 s, 1619 vs, 1576,

1505, 845 vs, 558 s. MS (ESI, CH_3CN, *m/z*): 312.7 ($[C_{62}H_{92}O_8N_{12}Ni_2]^{4+}$), 465.2 ($[C_{62}H_{92}O_8N_{12}Ni_2]^{4+} + PF_6^-$), 770.3 ($[C_{62}H_{92}O_8N_{12}Ni_2]^{4+} + 2PF_6^-$).

9Ni + 10Ni. MS (ESI, CH_3CN, *m/z*): 240.3 ($[C_{57}H_{90}N_{18}Ni_3]^{6+} - H^+$), 300.1 ($[C_{57}H_{90}N_{18}Ni_3]^{6+} - 2H^+$), 330.0 ($[C_{81}H_{122}O_8N_{18}Ni_3]^{6+}$ - H^+), 412.2 ($[C_{81}H_{122}O_8N_{18}Ni_3]^{6+}$ - $2H^+$).

(3,11,15,18,22,30,34,37,41,44,46,49-Dodecaazatricyclo[26.6.6.6^{13,20}]-pentaconta-1,12,14,18,20, 31,33,37,39,43,45,49-dodecaene-κ^8N)dicopper(II) Hexafluorophosphate (7Cu) and (3,11,15,18,22,30,34,-37,41,44,46,49-Dodecaazatricyclo[26.6.6.6^{13,20}]pentaconta-1,12,14,18,20,31,33,37,39,43,45,49-dodecaene-κ^8N)dicopper(II)-dibenzo-24-crown-8-[2] catenane Hexafluorophosphate (8Cu). 1,7-Heptanediamine (0.130 g, 1 mmol) and complex **2Cu** (0.630 g, 1 mmol) were separately dissolved in 100 mL of dry acetonitrile containing 0.448 g (1 mmol) dibenzo-24-crown-8. These two solutions were added at a rate of 15 $cm^3\ h^{-1}$, by means of a peristaltic pump, to a stirred solution of dibenzo-24-crown-8 (0.448 g, 1 mmol) in acetonitrile (100 mL). After the addition was complete, the solvent was removed by rotary evaporation to give a dark red residue. The residue was then washed out on top of a 2 cm × 25 cm acidic alumina column (Merck, activity I) with several small portions of chloroform. The column was washed with chloroform until all excessive crown ether was collected (∼1.2 g). The red solid remaining on the top of the column was then dissolved with a small volume of acetonitrile and eluted with the same solvent. The eluate was evaporated to dryness, and the solid was extracted several times with a dichloromethane−ethanol 10:1 solution. The remaining solid was then dissolved in acetonitrile, and this solution was filtered and diluted with ethanol. The bismacrocyclic complex (**7Cu**), precipitated upon evaporation of acetonitrile, was filtered off, washed with ethanol, and dried in vacuo. Yield: 0.150 g, 22%. The ethanol−dichloromethane solution was evaporated to dryness and the residue dissolved in acetonitrile and chromatographed on a 2 cm × 20 cm acidic alumina column with 5:1 dichloromethane−ethanol solution. After evaporation of the solvents, **8Cu** was crystallized upon slow evaporation of the acetonitrile−ethanol solution. Yield: 0.052 g, 5.5%.

7Cu. Anal. Calcd for $C_{38}H_{60}N_{12}Cu_2\cdot(PF_6)_4$ (1391.92): C, 32.8; H, 4.3; N, 12.1. Found: C, 32.8; H, 4.5; N, 11.8. MS (ESI, CH_3CN, *m/z*): 203.1 ($[C_{38}H_{60}N_{12}Cu_2]^{4+}$), 269.8 ($[C_{38}H_{60}N_{12}Cu_2]^{4+} - H^+$), 319.1 ($[C_{38}H_{60}N_{12}Cu_2]^{4+} + PF_6^-$), 551.1 ($[C_{38}H_{60}N_{12}Cu_2]^{4+} + 2PF_6^-$). IR (Nujol, cm^{-1}): 3370 m, 1662 w, 1617 vs, 1590 sh, 846 vs, 559 s.

8Cu. Anal. Calcd for $C_{62}H_{92}O_8N_{12}Cu_2\cdot(PF_6)_4\cdot 2H_2O$ (1876.47): C, 39.7; H, 5.2; N, 9.0. Found: C, 40.1; H, 5.4; N, 8.9. MS (ESI, CH_3CN, *m/z*): 315.1 ($[C_{62}H_{92}O_8N_{12}Cu_2]^{4+}$), 468.5 ($[C_{62}H_{92}O_8N_{12}Cu_2]^{4+} + PF_6^-$), 775.2 ($[C_{62}H_{92}O_8N_{12}Cu_2]^{4+} + 2PF_6^-$).

X-ray Diffraction. Single-crystal X-ray diffraction data were collected on KUMA (**5Ni**) and KUMA4CCD (**8Ni and 8Cu**) diffractometers with the use of graphite monochromated Mo Kα radiation. Data were collected at room (**5Ni**) temperature and at 100K (**8Ni** and **8Cu**) with a monocrystal cooled by a stream of cold nitrogen from an Oxford Cryosystems Cryostream cooler using $\omega-2\theta$ and ω scan techniques. Data reduction was carried out with the KUMARED software. No absorption correction was applied, but the data were corrected for Lorentz and polarization effects. The intensities of standard three reflections (**5Ni**) and a standard reference frame (**8Ni** and **8Cu**) were repeated every hour (**5Ni**) and every 25 frames collected (**8Ni** and **8Cu**). The program SHELXS[24] was used for structure solution, and the program SHELXL[25] for refinement. The refinement was based on F^2 for all reflections except those with very negative F^2. Weighted R factors wR and all goodness-of-fit *S* values are based on F^2. Conventional R factors are based on *F* with *F* set to zero for negative F^2. The $F_o^2 > 2\sigma(F_o^2)$ criterion was used only for calculating R factors and is not relevant to the choice of reflections for the refinement. The R factors based on F^2 are about twice as large as those based on *F*. Anisotropic temperature factors were used to describe the thermal motions of non-hydrogen atoms. Most of the hydrogen atoms were located in idealized averaged geometrical positions, allowed to ride at the heavy atoms and rotate around C−O and C−C bonds. For some of the non-hydrogen atoms of catenanes, only an isotropic model of atomic displacement parameters (ADPs) was applied. Additionally, we failed to find water hydrogen atoms. Atomic scattering factors for C, H, and O were derived from wave functions tabulated in Tables 6.1.1.4 and 4.2.4.2 from ref 26.

5Ni. $Ni_2C_{30}N_{12}H_{48}P_4F_{24}O_1$, fw = 1306; $T = 300$ K; $\lambda = 0.71073$ Å; orthorhombic; space group, *Pbca*; unit cell dimensions, $a = 18.145(4)$ Å, $b = 14.512(3)$ Å, $c = 18.623(4)$ Å, vol = 4904(2) $Å^3$; $Z = 4$; density (calcd) = 1.77 Mg/m^3; absorption coefficient = 1.04 mm^{-1}; $F(000) = 2640$; crystal size = 0.30 × 0.20 × 0.20 mm^3; θ range for data collection = 2.1−21°; index ranges: $-1 \le h \le 18$, $-1 \le k \le 14$, $-18 \le l \le 1$; reflections collected = 3345; independent reflections = 2627 [$R_{int} = 0.029$]; refinement method, full-matrix least-squares on F^2; data/restraints/parameters = 2627/0/422; goodness-of-fit on $F^2 = 0.958$; final R indices [$I > 2\sigma(I)$]: R1 = 0.0460 and wR2 = 0.1164; R indices (all data): R1 = 0.1002, wR2 = 0.1449, extinction coefficient = 0; weight = $1/[\sigma^2(F_o^2) + (0.0747P)^2 + 12.95P]$ where $P = (\mathrm{Max}(F_o^2, 0) + 2F_c^2)/3$; largest diffraction peak and hole = 0.543 and −0.347 e A^{-3}.

8Ni. $Ni_2C_{62}N_{12}H_{93}P_4F_{24}O_{10}$, fw = 1863.78; $T = 100$ K; $\lambda = 0.71073$ Å; monoclinic; space group $P2_1/c$; unit cell dimensions, $a = 11.349(2)$ Å, $b = 43.558(9)$ Å, $c = 16.546(3)$ Å, β =93.05(3)°;

vol = 8168(3) $Å^3$; $Z = 4$; density(calcd) = 1.516 Mg/m^3; absorption coefficient = 0.654 mm^{-1}; $F(000) = 3844$; crystal size = 0.35 × 0.15 × 0.06 mm^3; θ range for data collection = 3.65−20.5°; index ranges: $-11 \le h \le 11$, $-42 \le k \le 42$, $-16 \le l \le 16$; reflections collected = 61 690; independent reflections = 8146 [$R_{int} = 0.286$]; refinement method, full-matrix least-squares on F^2; data/restraints/parameters = 8146/0/1023; goodness-of-fit on $F^2 = 1.047$; final R indices [$I > 2\sigma(I)$]: R1 = 0.1295 and 0.1803 for all data, wR2 = 0.2887; extinction coefficient = 0.0011(3); weight = $1/[\sigma^2(Fo^2) + (0.1329P)^2 + 98.05P]$ where $P = (\mathrm{Max}(F_o^2, 0) + 2F_c^2)/3$; largest diffraction peak and hole = 1.177 and −0.654 e A^{-3}.

8Cu. $Cu_2C_{62}N_{12}H_{94}P_4F_{24}O_{10}$, fw = 1873.45; $T = 100$ K; $\lambda = 0.71073$ Å; monoclinic; space group $P2_1/n$; unit cell dimensions: $a = 21.725(4)$ Å, $b = 14.224(3)$ Å, $c = 28.684(6)$ Å, $\beta = 112.21(3)$°; vol = 8206(3) $Å^3$; $Z = 4$; density(calcd) = 1.517 Mg/m^3; absorption coefficient = 0.71 mm^{-1}; $F(000) = 3856$; crystal size = 0.20 × 0.10 × 0.06 mm^3; θ range for data collection = 3.65−22.50°; index ranges: $-23 \le h \le 23$, $-15 \le k \le 15$, $-30 \le l \le 30$; reflections collected = 96 341; independent reflections = 10 707 [$R_{int} = 0.3742$]; refinement method: full-matrix least-squares on F^2; data/restraints/parameters = 10 707/0/958; goodness-of-fit on $F^2 = 1.131$; final R indices [$F > 3.5\sigma(F)$]: R1 = 0.149 and 0.2724 for all data, wR2 = 0.3713; weight = $1/[\sigma^2(F_o^2) + (0.1298P)^2]$ where $P = (\mathrm{Max}(F_o^2, 0) + 2F_c^2)/3$; largest diffraction peak and hole = 0.88 and −0.47 e A^{-3}.

Crystallographic data (excluding structural factors) for the structures reported in this paper have been deposited with the Cambridge Crystallographic Data Center and allocated the deposition numbers CCDC 160915, CCDC 160916, and CCDC 160917 for **5Ni, 8Ni**, and **8Cu,** respectively. Copies of the data can be obtained free of charge on application to CCDC, 12 Union Road, Cambridge CB2 1EW, U.K. (Fax: Int code + (1223)336-033. E-mail: deposit@ccdc.cam.ac.uk).

Voltammetry. Voltammetric experiments were done using the Autolab potentiostat (ECO Chemie, Netherlands) or an EG&G PARC Model 273 potentiostat controlled via ECHEM software on a PC486 computer. The COOL algorithm was used to fit the experimental curves to an *E*1*E*2 mechanism and to obtain the potentials of individual electron transfers.[27,28] A three electrode arrangement with a Ag/AgCl electrode as the reference, platinum foil as the counter, and glassy carbon electrode (GCE, BAS, 3 mm diameter) as the working electrode was used. The reference electrode was separated from the working solution by an electrolytic bridge. The acetonitrile (AN) containing 0.1 M tetrabutylammonium hexafluorophosphate (TBAHFP) was used as the supporting electrolyte solution. The potential of the reference electrode was calibrated by using the ferrocene oxidation process in the same TBAHFP/AN solution. Experiments were done at 25 °C in solutions

(24) Sheldrick, G. M. *Acta Crystallogr*. **1990**, *A 46*, 467.

(25) Sheldrick, G. M. *SHELXL93: Program for the Refinement of Crystal Structures*; University of Gottingen: Gottingen, 1993.

(26) *International Tables for Crystallography*; Wilson, A. J. C., Ed.; Kluwer: Dordrecht, 1992, Vol. C.

(27) *Model 271 COOL*, Kinetic Analysis Software, Users Guide; EG&G Instruments Cooperation, 1992.

(28) Słowiński, K.; Bilewicz, R.; Kublik, Z.; Pietraszkiewicz, M. *Pol. J. Chem.*, **1995**, *69*, 707−715.

deaerated by passing argon, and an argon blanket was maintained over the solution during the measurements.

Acknowledgment. This work was financially supported by the State Committee for Scientific Research (Project 3 T09A 076 15). R.B. and K.W. acknowledge support from the MNEMON Project (KBN 3 T09A 098 14). The X-ray measurements were made in the Crystallographic Unit of the Physical Chemistry Laboratory at the Chemistry Department of the University of Warsaw.

Supporting Information Available: ESI mass spectrometry results (Table S1 and Figure S1), numerical information regarding the shortest intermolecular contacts for **5Ni, 8Ni**, and **8Cu (**Tables S2−S4 and Figures S2−S4, respectively), crystal packing of molecules (Figure S5), and a plot illustrating experimental and fitted cyclic voltammograms for **8Cu** (Figure S6). This material is available free of charge via the Internet at http://pubs.acs.org.

JA0108537